Monthly Notices
of the
ROYAL ASTRONOMICAL SOCIETY

MNRAS **465,** 5011–5015 (2017)
Advance Access publication 2016 December 5

doi:10.1093/mnras/stw3105

Giant Metrewave Radio Telescope detection of associated H I 21-cm absorption at $z = 1.2230$ towards TXS 1954+513

J. N. H. S. Aditya,[1⋆] Nissim Kanekar,[1⋆†] J. Xavier Prochaska,[2] Brandon Day,[3] Paul Lynam[2] and Jocelyn Cruz[4]

[1]*National Centre for Radio Astrophysics, Tata Institute of Fundamental Research, Pune 411007, India*
[2]*UCO/Lick Observatory, University of California – Santa Cruz, Santa Cruz, CA 95064, USA*
[3]*Department of Physics, University of California – Santa Cruz, Santa Cruz, CA 95064, USA*
[4]*Department of Astrononomy and Astrophysics, University of California – Santa Cruz, Santa Cruz, CA 95064, USA*

Accepted 2016 November 28. Received 2016 October 27; in original form 2016 July 21

ABSTRACT

We have used the 610-MHz receivers of the Giant Metrewave Radio Telescope (GMRT) to detect associated H I 21-cm absorption from the $z = 1.2230$ blazar TXS 1954+513. The GMRT H I 21-cm absorption is likely to arise against either the milliarcsecond-scale core or the one-sided milliarcsecond-scale radio jet, and is blueshifted by $\approx$328 km s^{-1} from the blazar redshift. This is consistent with a scenario in which the H I cloud giving rise to the absorption is being driven outwards by the radio jet. The integrated H I 21-cm optical depth is (0.716 ± 0.037) km s^{-1}, implying a high H I column density, $N_{\rm HI} = (1.305 \pm 0.067) \times (T_{\rm s}/100\,{\rm K}) \times 10^{20}$ cm^{-2}, for an assumed H I spin temperature of 100 K. We use Nickel Telescope photometry of TXS 1954+513 to infer a high rest-frame 1216 Å luminosity of $(4.1 \pm 1.2) \times 10^{23}$ W Hz^{-1}. The $z = 1.2230$ absorber towards TXS 1954+513 is only the fifth case of a detection of associated H I 21-cm absorption at $z > 1$, and is also the first case of such a detection towards an active galactic nucleus (AGN) with a rest-frame ultraviolet (UV) luminosity $\gg 10^{23}$ W Hz^{-1}, demonstrating that neutral hydrogen can survive in AGN environments in the presence of high UV luminosities.

Key words: galaxies: active – galaxies: high-redshift – quasars: absorption lines – radio lines: galaxies.

1 INTRODUCTION

'Associated' H I 21-cm absorption studies have been used to probe physical conditions in neutral atomic hydrogen (H I) in the environments of active galactic nuclei (AGNs) for more than four decades (e.g. Roberts 1970). Such studies allow one to trace the presence and kinematics of, as well as physical conditions in, H I in AGN environments as a function of redshift and AGN type. For example, comparisons between the H I 21-cm absorption redshift and the AGN emission redshift allow one to determine whether the detected absorption arises from gas outflow or infall, and thus to study the fuelling of the active nucleus or the effects of AGN feedback (e.g. Morganti, Tadhunter & Oosterloo 2005b; Morganti et al. 2013). One can also use such observations, especially with very long baseline interferometry (VLBI) techniques, to study the kinematics of circumnuclear discs around AGNs (e.g. Conway & Blanco 1995; Peck & Taylor 2002), interactions between the active nucleus, the radio jet and the ambient gas (e.g. Morganti et al. 2005a), and even to infer the presence of binary supermassive black holes in active galaxies (e.g. Morganti et al. 2009). The detectability of such associated H I 21-cm absorption in different AGN types can also be used to test AGN unification schemes (e.g. Barthel 1989).

More than a hundred radio-loud AGNs have been searched for associated H I 21-cm absorption, from local systems out to very high redshifts, $z \approx 5.2$ (e.g. van Gorkom et al. 1989; Vermeulen et al. 2003; Gupta et al. 2006; Carilli et al. 2007; Curran et al. 2008; Geréb et al. 2015; Aditya, Kanekar & Kurapati 2016). More than 50 associated systems have been detected in H I 21-cm absorption till now, with the vast majority at low redshifts, $z \lesssim 0.7$ (e.g. Vermeulen et al. 2003; Gupta et al. 2006; Geréb et al. 2015), and, indeed, only four confirmed detections at $z > 1$ (Uson, Bagri & Cornwell 1991; Moore, Carilli & Menten 1999; Ishwara-Chandra, Dwarakanath & Anantharamaiah 2003; Curran et al. 2013). While this might suggest redshift evolution in the neutral gas content in AGN environments, the heterogeneity of most target samples, with typically a mix of compact and extended background radio sources, has meant that it has been difficult to separate the AGN characteristics from the above redshift evolution. It has also been pointed out that H I 21-cm absorption has never been detected in the environment of an AGN with a rest-frame ultraviolet (UV) luminosity $\gtrsim 10^{23}$ W Hz^{-1},

⋆ E-mail: adityaj@iucaa.in (JNHSA); nkanekar@ncra.tifr.res.in (NK)
† Swarnajayanti Fellow.

at either low or high redshifts (Curran et al. 2008). These authors argue that the above luminosity may be a threshold above which neutral gas does not survive in AGN environments.

The two main problems with using H I 21-cm absorption to probe the redshift evolution of AGN environments have been the lack of searches for H I 21-cm absorption at high redshifts, $z > 1$, and the heterogeneity in the target samples at all redshifts. We have hence been using the Giant Metrewave Radio Telescope (GMRT) to carry out a search for redshifted H I 21-cm absorption in a large, uniformly selected sample of compact sources, the Caltech–Jodrell flat-spectrum sample (Pearson & Readhead 1988; Taylor et al. 1996). Our pilot study of a subset of this sample yielded the first statistically significant evidence for redshift evolution in the detectability of associated H I 21-cm absorption in a uniformly selected sample (Aditya et al. 2016). However, the data are also consistent with a scenario in which AGNs with a high UV or radio luminosity have a lower H I 21-cm absorption strength, as suggested by Curran et al. (2008). In this study, we report a new detection of redshifted H I 21-cm absorption from our GMRT survey of flat-spectrum radio sources, at $z \approx 1.2230$, towards TXS 1954+513, the first case of associated H I 21-cm absorption in a UV-luminous quasar.

2 THE TARGET: TXS 1954+513

TXS 1954+513 is classified as a blazar in the literature (e.g. Xie, Dai & Zhou 2007; Healey et al. 2008; Massaro et al. 2009), based on its optical, X-ray and radio characteristics. Specifically, the optical spectrum shows broad emission lines (Lawrence et al. 1996), the source has a high X-ray luminosity ($>10^{43}$ erg s^{-1}; Britzen et al. 2007), the low-frequency radio spectrum is very flat (with a spectral index of $\alpha = 0.01$ between 1.4 and 5 GHz) and the radio flux density varies on time-scales of a few days (Heeschen 1984), all typical blazar properties.

The redshift of TXS 1954+513 has been estimated to be $z = 1.2230$ (Lawrence et al. 1996), based on the detection of a slew of both broad and narrow emission lines (including O II λ3727, O III λ4363, H γ, H δ, etc.). The large number of detected lines allows an accurate estimate of the AGN redshift: Lawrence et al. (1996) estimate the redshift uncertainty to be $\approx$0.0001 for this source.

Unfortunately, there are few optical photometric studies of TXS 1954+513 in the literature. Monet et al. (2003) obtain $R = 17.34$ and $B = 18.87$ from the second epoch of the USNO-B catalogue, with slightly different values ($R = 17.47$ and $B = 18.44$) in the first epoch. This would imply a high inferred rest-frame 1216 Å luminosity (e.g. Curran et al. 2008). However, the errors on the above measurements are uncertain (Monet et al. 2003); we hence chose to also carry out optical imaging of TXS 1954+513 to obtain accurate photometry.

3 OBSERVATIONS, DATA ANALYSIS AND RESULTS

3.1 GMRT imaging and spectroscopy

The GMRT was initially used to search for associated redshifted H I 21-cm absorption towards TXS 1954+513 in 2014 April, using the 610-MHz receivers and the GMRT software backend was used as the correlator. A bandwidth of 16.7 MHz was used for the observations, centred at the expected redshifted H I 21-cm line frequency ($\approx$638.96 MHz) and subdivided into 512 channels; this yielded a velocity resolution of $\approx$15.3 km s^{-1} and a total velocity coverage of $\approx$7815 km s^{-1} (covering redshifts $z \approx 1.194$–1.252). Observations of the standard calibrators 3C286 and 3C295 were used to calibrate the flux density scale and the system passband. No phase calibrator was observed as TXS 1954+513 is known to be relatively compact at low frequencies. The on-source time was $\approx$60 min.

The spectrum from the original GMRT observations showed statistically significant evidence for a narrow absorption feature close to the expected redshifted H I 21-cm line frequency. We hence re-observed TXS 1954+513 in 2015 May to confirm the detection, again using the GMRT software backend was used as the correlator, but this time with a bandwidth of 4.17 MHz sub-divided into 512 channels, and centred at the redshifted H I 21-cm line frequency. This yielded a finer velocity resolution of $\approx$3.8 km s^{-1}, allowing us to resolve out any narrow spectral components in the absorption profile. 3C286 was again used to calibrate the flux density scale and the system bandpass. The on-source time was $\approx$90 min.

3.2 Nickel Telescope photometry

The field surrounding TXS 1954+513 was imaged through the *B* and *R* filters using the 1-m Nickel Telescope at the Lick Observatory on UT 2016 September 14. Images of 600 and 1800 s were obtained under clear but humid conditions. Images of the standard fields PG2213-006 and SA 111 (Landolt 2009) were taken directly after the science field for photometric calibration. Additional calibration frames (bias, dome flats) were also obtained. Image processing of the on-sky images proceeded in a standard fashion (e.g. bias subtraction, flat-field normalization) with custom scripts.

We measured the counts in 14-arcsec-diameter apertures around each calibration star and estimated the sky counts from a nearby, off-source aperture. The measured zero-points corresponding to 1 count s^{-1} are $ZP_B = 22.1$ mag and $ZP_R = 22.7$ mag, for the *B* and *R* filters, respectively. Aperture photometry was then performed on TXS 1954+513; after applying the zero-point corrections, we obtained $B = 18.0$ mag and $R = 16.9$ mag, on the Vega magnitude scale. We estimate an uncertainty of 0.15 mag from calibration errors and photon statistics.

3.3 Data analysis and results

The GMRT data on TXS 1954+513 were analysed in 'classic' AIPS following standard procedures. The data were first carefully inspected, and edited to remove non-working antennas and time-specific intermittent bad data (e.g. due to radio frequency interference). The antenna bandpasses were estimated from the data on the bright calibrators 3C286 and 3C295. An initial estimate of the complex antenna gains was obtained by assuming TXS 1954+513 to be a point source, and the gains were then refined via an iterative self-calibration procedure consisting of four rounds of phase-only self-calibration and imaging, followed by two rounds of amplitude-and-phase self-calibration and imaging. The amplitude-and-phase self-calibration step was followed by further data editing, based on the residuals after subtracting the continuum image from the calibrated visibilities. This iterative procedure was carried out until it yielded an image that did not improve upon further self-calibration and data editing. The final continuum image was then subtracted out from the calibrated spectral-line visibilities; any remaining continuum emission was removed by fitting a first-order polynomial to line-free channels in each visibility spectrum, and subtracting this out. The residual visibilities were then shifted to the heliocentric frame, and imaged to obtain the final spectral cube.

The final GMRT 640-MHz continuum image of TXS 1954+513, displayed in Fig. 1, shows a central core and two emission

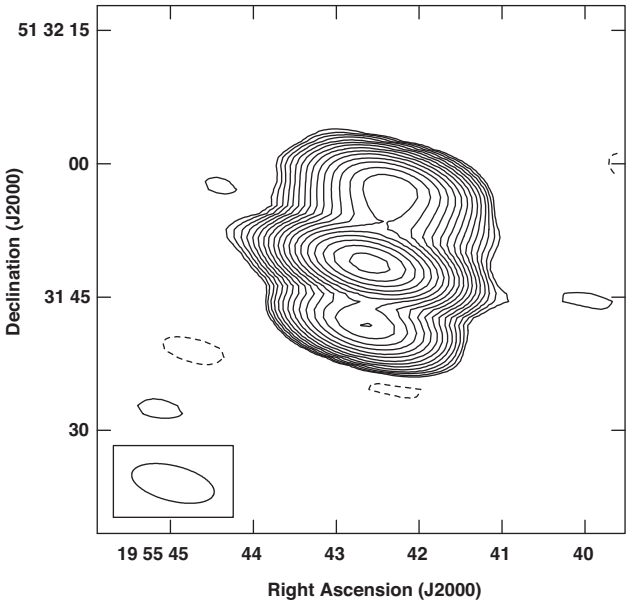

Figure 1. The GMRT 640-MHz continuum image of TXS 1954+513, showing the core-dominated triple structure. The positive contour levels extend from 2 to 512 mJy, in steps of $\sqrt{2}$, while the sole negative (dashed) contour is at −2 mJy. The peak continuum flux is 1.221 30 ± 0.000 69 Jy beam^{-1}, and the synthesized beam has a full width at half-maximum of 10.6 × 4.4 arcsec^2.

components extended in the north and south directions. A three-component Gaussian model was fitted to the GMRT image (using the task JMFIT) to measure the flux densities of the three components; this yielded flux densities of (1254.1 ± 1.2) (core), (403.4 ± 1.6) (northern lobe) and (198.1 ± 1.3) mJy (southern lobe). The core emission is marginally resolved, with a peak flux of (1221.30 ± 0.69) mJy beam^{-1}, the northern lobe is highly resolved, with a peak flux of (247.90 ± 0.66) mJy beam^{-1}, while the southern lobe is also marginally resolved, with a peak flux of (184.00 ± 0.69) mJy beam^{-1}.

The radio core dominates the emission, providing ≈70 per cent of the total flux density at our observing frequency of 640 MHz; as a result, the spectrum remains relatively flat at low frequencies, with a spectral index $\alpha \approx -0.2$ between 640 MHz and 1.4 GHz (Condon et al. 1998) obtained from the total flux densities at the two frequencies (assuming the flux density S_ν at a frequency ν to be given by $S_\nu \propto \nu^\alpha$). The angular size of the source in the north–south direction is ≈20 arcsec, i.e. ≈170 kpc at the AGN redshift of $z = 1.2230$.

The three panels of Fig. 2 show H I 21-cm spectra at the locations of the peaks of the three emission components of TXS 1954+513 (after subtracting out a second- or third-order baseline fitted to line-free regions), with optical depth (in units of 1000 × τ) plotted versus velocity (in km s^{-1}), relative to the heliocentric redshift $z = 1.2230$. These were obtained from the second observing run in 2015 May, whose data have both a better spectral resolution and a higher sensitivity. Strong H I 21-cm absorption is clearly visible in the spectrum through the radio core, shown in the left-hand panel, while no H I 21-cm absorption was detected in the spectra through the two lobes, shown in the middle and right-hand panels of the figure. Note that the optical-depth sensitivities of the spectra towards the peaks of the northern and southern lobes are sufficient to detect H I 21-cm absorption of the same strength as that of the main absorption component seen against the core but not to detect the weaker absorption component. We can thus rule out the possibility that the 'cloud' producing the strong H I 21-cm absorption covers both the core and either of the lobes but cannot rule out the possibility that the gas producing the weaker H I 21-cm absorption might cover all three source components.

The root-mean-square noise on the spectrum through the core was measured (from line-free channels) to be ≈2.3 mJy per 3.8 km s^{-1} channel. The integrated H I 21-cm optical depth of the absorption line detected against the core is (0.716 ± 0.037) km s^{-1}, which implies an H I column density of $N_{\rm HI} = (1.305 \pm 0.067) \times (T_{\rm s}/100\,{\rm K}) \times 10^{20}$ cm^{-2}, for an assumed spin temperature of 100 K (this value was used for consistency with the literature; e.g. Vermeulen et al. 2003; Gupta et al. 2006). Note that the spin temperature of neutral hydrogen in AGN environments could be much higher than the assumed 100 K (e.g. Maloney, Hollenbach & Tielens 1996); the above estimate of the H I column density is hence likely to be a lower limit.

The detected H I 21-cm absorption towards the core of TXS 1954+513 is relatively narrow, with a velocity width between 20 per cent points of ≈40 km s^{-1}. No evidence is seen for a wide absorption component. The peak of the absorption is blueshifted from the AGN redshift ($z = 1.2230 \pm 0.0001$; Lawrence et al. 1996) by ≈328 km s^{-1}.

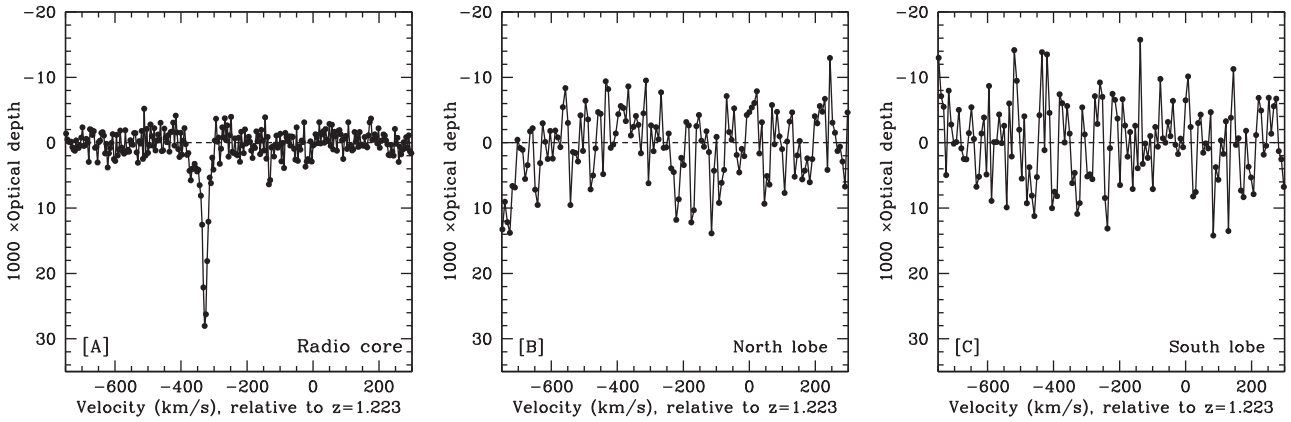

Figure 2. GMRT H I 21-cm absorption spectra towards (A) (left-hand panel) the radio core, (B) (middle panel) the northern lobe and (C) (right-hand panel) the southern lobe. In all three spectra, optical depth (in units of 1000 × τ) is plotted against velocity, in km s^{-1}, relative to the AGN redshift of $z = 1.2230$. It is clear that the optical-depth sensitivity towards the two lobes is sufficient to detect H I 21-cm absorption of the same strength as that seen towards the radio core.

4 DISCUSSION

A clear core-jet structure is seen on scales of tens of milliarcseconds in the 1.6-GHz VLBI image of TXS 1954+513, with a single jet in the eastward direction (Polatidis et al. 1995). The one-sided nature of the jet indicates that it is likely to point close to our line of sight to the core. Interestingly, however, our GMRT 640-MHz continuum image shows that the radio structure is very different on arcsecond scales, with a core and two weaker lobes symmetrically extended in the north–south direction with a transverse angular extent of ≈25 arcsec; this three-component north–south structure is also seen in the 1.4-GHz Very Large Array image of Xu et al. (1995). The arcsecond-scale structure is thus of the 'core-dominated triple' type (e.g. Marecki et al. 2006). However, the milliarcsecond scale core-jet structure is nearly perpendicular to the north–south arcsecond-scale structure. Such strong misalignments between the milliarcsecond-scale and the arcsecond-scale radio structures have been observed earlier in a number of AGNs, especially BL Lac objects (e.g. Pearson & Readhead 1988; Wehrle et al. 1992; Conway & Murphy 1993), and, more recently, in a few core-dominated triples (e.g. Marecki et al. 2006). Models that can account for these misalignments include twisted radio jets, either due to the interaction with the ambient medium or due to the precession of the axis of the central supermassive black hole (e.g. Conway & Murphy 1993; Appl, Sol & Vicente 1996), and restarted AGN activity accompanied by a flip in the spin of the central black hole, possibly due to a galaxy merger event (e.g. Marecki et al. 2006).

We followed the prescription of Curran et al. (2008) to estimate the rest-frame UV luminosity of TXS 1954+513, using a power-law model to extrapolate from its measured *R*-band and *B*-band magnitudes to infer its flux density at $1216 \times (1 + z)$ Å ($z = 1.223$), and, hence, its luminosity at this wavelength. Our measured *R*-band and *B*-band magnitudes are $R = 16.9 \pm 0.15$ and $B = 18.0 \pm 0.15$. Extrapolating from these measurements, we obtain $L_{\rm UV} \approx (4.1 \pm 1.2) \times 10^{23}$ W Hz^{-1}; this is by far the highest UV luminosity at which associated H I 21-cm absorption has been detected at any redshift (e.g. Curran et al. 2008, 2010). This is also the first case of a detection of H I 21-cm absorption above the UV luminosity threshold suggested by Curran et al. (2010) of $L_{\rm UV} = 10^{23}$ W Hz^{-1}. Curran & Whiting (2012) use a simple model to argue that this is the UV luminosity threshold above which a quasar would ionize all the neutral gas in its host galaxy, for a range of gas densities. Our detection of H I 21-cm absorption shows that neutral hydrogen can indeed survive in AGN environments at high UV luminosities, $\gg 10^{23}$ W Hz^{-1}.

The peak of the H I 21-cm absorption is blueshifted by ≈328 km s^{-1} from the AGN redshift of 1.2230, indicating that this is a case of gas outflow from an AGN. The detected absorption against the core of the GMRT 640-MHz image may arise against either the VLBI core or the VLBI scale, eastward-pointing radio jet of TXS 1954+513. However, since the jet direction is likely to lie close to our line of sight to the core, in both cases the gas cloud appears to be moving in the direction of the VLBI radio jet and away from the core. It is possible that the neutral gas in the vicinity of the AGN is being driven outwards by the ram pressure of the radio jet, as has been suggested by recent numerical simulations (e.g. Wagner & Bicknell 2011; Wagner, Bicknell & Umemura 2012).

In summary, we have used the GMRT 610-MHz receivers to obtain only the fifth detection of associated redshifted H I 21-cm absorption at high redshifts, $z > 1$, in the blazar TXS 1954+513. The AGN has a core-dominated triple structure in the GMRT image, with the two radio lobes oriented nearly perpendicular to the VLBI-scale radio jet; this misalignment may arise due to either a twisted radio jet or restarted AGN activity with a spin-flip of the central black hole. The H I 21-cm absorption is detected towards the radio core of the GMRT 640-MHz image, i.e. towards either the VLBI core or the VLBI-scale radio jet, and is blueshifted by ≈328 km s^{-1} from the AGN redshift, suggesting that the H I cloud causing the absorption is being driven outwards by the ram pressure of the jet. We have also used Nickel Telescope *R*- and *B*-band photometry of TXS 1954+513 to infer a high rest-frame 1216-Å luminosity of $(4.1 \pm 1.2) \times 10^{23}$ W Hz^{-1} for the blazar. This is the first case of associated H I 21-cm absorption detected from an AGN with a rest-frame UV luminosity $>10^{23}$ W Hz^{-1}, showing that neutral gas can survive in the vicinity of AGNs with high UV luminosities.

ACKNOWLEDGEMENTS

We thank the staff of the GMRT who have made these observations possible. The GMRT is run by the National Centre for Radio Astrophysics of the Tata Institute of Fundamental Research. NK acknowledges support from the Department of Science and Technology via a Swarnajayanti Fellowship (DST/SJF/PSA-01/2012-13).

REFERENCES

Aditya J. N. H. S., Kanekar N., Kurapati S., 2016, MNRAS, 455, 4000
Appl S., Sol H., Vicente L., 1996, A&A, 310, 419
Barthel P. D., 1989, ApJ, 336, 606
Britzen S. et al., 2007, A&A, 472, 763
Carilli C. L. et al., 2007, ApJ, 666, L9
Condon J. J., Cotton W. D., Greisen E. W., Yin Q. F., Perley R. A., Taylor G. B., Broderick J. J., 1998, AJ, 115, 1693
Conway J. E., Blanco P. R., 1995, ApJ, 449, L131
Conway J. E., Murphy D. W., 1993, ApJ, 411, 89
Curran S. J., Whiting M. T., 2012, ApJ, 759, 117
Curran S. J., Whiting M. T., Wiklind T., Webb J. K., Murphy M. T., Purcell C. R., 2008, MNRAS, 391, 765
Curran S. J., Tzanavaris P., Darling J. K., Whiting M. T., Webb J. K., Bignell C., Athreya R., Murphy M. T., 2010, MNRAS, 402, 35
Curran S. J., Whiting M. T., Sadler E. M., Bignell C., 2013, MNRAS, 428, 2053
Geréb K., Maccagni F. M., Morganti R., Oosterloo T. A., 2015, A&A, 575, 44
Gupta N., Salter C. J., Saikia D. J., Ghosh T., Jeyakumar S., 2006, MNRAS, 373, 972
Healey S. E. et al., 2008, ApJS, 175, 97
Heeschen D. S., 1984, AJ, 89, 1111
Ishwara-Chandra C. H., Dwarakanath K. S., Anantharamaiah K. R., 2003, JA&A, 24, 37
Landolt A. U., 2009, AJ, 137, 4186
Lawrence C. R., Zucker J. R., Readhead A. C. S., Unwin S. C., Pearson T. J., Xu W., 1996, ApJS, 107, 541
Maloney P. R., Hollenbach D. J., Tielens A. G. G. M., 1996, ApJ, 466, 561
Marecki A., Thomasson P., Mack K.-H., Kunert-Bajraszewska M., 2006, A&A, 448, 479
Massaro E., Giommi P., Leto C., Marchegiani P., Maselli A., Perri M., Piranomonte S., Sclavi S., 2009, A&A, 495, 691
Monet D. G. et al., 2003, AJ, 125, 984
Moore C. B., Carilli C. L., Menten K. M., 1999, ApJ, 510, L87
Morganti R., Oosterloo T. A., Tadhunter C. N., van Moorsel G., Emonts B., 2005a, A&A, 439, 521
Morganti R., Tadhunter C. N., Oosterloo T. A., 2005b, A&A, 444, L9
Morganti R., Peck A. B., Oosterloo T. A., van Moorsel G., Capetti A., Fanti R., Parma P., de Ruiter H. R., 2009, A&A, 505, 559

Morganti R., Fogasy J., Paragi Z., Oosterloo T., Orienti M., 2013, Science, 341, 1082
Pearson T. J., Readhead A. C. S., 1988, ApJ, 328, 114
Peck A. B., Taylor G. B., 2002, New Astron. Rev., 46, 273
Polatidis A. G., Wilkinson P. N., Xu W., Readhead A. C. S., Pearson T. J., Taylor G. B., Vermeulen R. C., 1995, ApJS, 98, 1
Roberts M. S., 1970, ApJ, 161, L9
Taylor G. B., Vermeulen R. C., Readhead A. C. S., Pearson T. J., Henstock D. R., Wilkinson P. N., 1996, ApJS, 107, 37
Uson J. M., Bagri D. S., Cornwell T. J., 1991, Phys. Rev. Lett., 67, 3328
van Gorkom J. H., Knapp G. R., Ekers R. D., Ekers D. D., Laing R. A., Polk K. S., 1989, AJ, 97, 708
Vermeulen R. C. et al., 2003, A&A, 404, 861
Wagner A. Y., Bicknell G. V., 2011, ApJ, 728, 29
Wagner A. Y., Bicknell G. V., Umemura M., 2012, ApJ, 757, 136
Wehrle A. E., Cohen M. H., Unwin S. C., Aller H. D., Aller M. F., Nicolson G., 1992, ApJ, 391, 589
Xie G. Z., Dai H., Zhou S. B., 2007, AJ, 134, 1464
Xu W., Readhead A. C. S., Pearson T. J., Polatidis A. G., Wilkinson P. N., 1995, ApJS, 99, 297

This paper has been typeset from a TEX/LATEX file prepared by the author.